Inorganic Chemistry

Article

pubs.acs.org/IC

Self-Assembly of Discrete M_6L_8 Coordination Cages Based on a Conformationally Flexible Tripodal Phosphoric Triamide Ligand

Xing-Jun Li,[†,‡] Fei-Long Jiang,[†] Ming-Yan Wu,[†] Shu-Quan Zhang,[†] You-Fu Zhou,[†] and Mao-Chun Hong*[,†]

[†]State Key Laboratory of Structural Chemistry, Fujian Institute of Research on the Structure of Matter, Chinese Academy of Sciences, Fuzhou, Fujian 350002, People's Republic of China

[‡]Graduate University, Chinese Academy of Sciences, Beijing 100039, People's Republic of China

Supporting Information

ABSTRACT: Reactions of a tripodal ligand, *N*,*N*′,*N*″-tris(3-pyridinyl)phosphoric triamide (TPPA), and a series of transition-metal ions result in the assembly of five discrete M_6L_8 coordination cages $[M_6(TPPA)_8(H_2O)_{12}](ClO_4)_{12}\cdot 57H_2O$ [M = Ni^{2+} (**1**), Co^{2+} (**2**), Zn^{2+} (**3**), Cd^{2+} (**4**)] and $[Pd_6(TPPA)_8]Cl_{12}\cdot 22H_2O$ (**5**). X-ray structural analyses reveal that the cages have large internal cavities and flexible windows. The flexible ligand TPPA adopts the syn conformation in cages **1**−**4**, but it transforms to the anti conformation in cage **5**. Because of the conformational transformation, the sizes of the windows and the volume of the internal cavity of cage **5** are increased. ^{1}H NMR and electrospray mass spectrometric studies show that cage **5** maintains its structural integrity in solution. Additionally, compounds **3** and **4** exhibit strong blue fluorescent emissions, which are 1 order of magnitude higher than that of the free ligand.

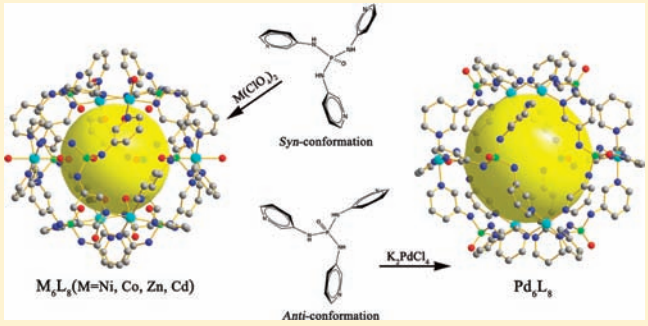

INTRODUCTION

Self-assembled coordination cages have attracted much attention because of their fascinating structures and intriguing applications such as recognition,[1] delivery,[2] catalysis,[3] separation, and gas storage.[4] During the past few decades, extensive studies have been made on discrete molecular assemblies M_xL_y with various values of x and y.[5] Among these discrete metal−ligand assemblies, the self-assembled M_6L_8 coordination cage is an important species.[6] A useful strategy for obtaining this kind of cage is the use of triangular facial ligands to link metal ions with octahedral or square-planar coordination geometry. The flexibility of the ligand is essential for the formation of a discrete M_6L_8 cage because it allows the ligand adopting variable conformations to meet the requirement of coordination geometries of metal ions in the assembly process. It is feasible to reduce the rigidness of the ligand by introducing some functional groups, such as −NH−, $-CH_2-$, −S−, and −O−, to the ligand. The resulting coordinated complexes usually have an octahedral or spherical structure in which six metal ions lie on the apexes and eight ligands occupy the eight sides. By using this strategy, several discrete M_6L_8 cages have been successfully synthesized. For instance, Fujita and co-workers combined a tripodal tridentate ligand with $Pd(NO_3)_2$ to form a hollow M_6L_8 molecular sphere.[6a] Lah and co-workers reported two nanosized octahedral cages using suitably designed C_3-symmetric triangular ligands as facial components and C_4-symmetric Pd^{II} metal ions as corner linkers.[6b] In our previous studies, we synthesized a neutral M_6L_8 metallosupramolecular cube cage based on a flexible pyridine-based ligand and octahedral Ni^{II} ions.[6c]

Keeping this strategy in mind, we designed a new flexible tripodal ligand, *N*,*N*′,*N*″-tris(3-pyridinyl)phosphoric triamide (denoted as TPPA hereafter), to attempt to build discrete M_6L_8 cages. The C_3-symmetric ligand TPPA, which was synthesized in high yield from the reaction of 3-aminopyridine and phosphoryl chloride, possesses three pyridine rings connecting a phosphoryl group via flexible amide units. As expected, the pyridine rings can freely rotate around the amide functional groups, which allow the ligand to adopt different conformations and satisfy the coordination requirements of different metal centers. It is notable that the amide functional groups of the ligands would form hydrogen bonds with appropriate solvent molecules, thus improving the solubility of the resultant molecular cages.

Herein, we report the assembly of five octahedral M_6L_8 cages constructed by the conformationally flexible tripodal ligand TPPA, namely, $[M_6(TPPA)_8(H_2O)_{12}](ClO_4)_{12}\cdot 57H_2O$ [M = Ni^{2+} (**1**), Co^{2+} (**2**), Zn^{2+} (**3**), Cd^{2+} (**4**)] and $[Pd_6(TPPA)_8]Cl_{12}\cdot 22H_2O$ (**5**). Interestingly, the flexible ligand TPPA adopts two different conformations in cages **1**−**4** and cage **5**, respectively, denoted as the syn and anti conformations. When the pyridyl N and phosphoryl O of the ligand are on the same side, the conformation of the ligand is defined as syn.

Received: November 3, 2011
Published: March 22, 2012

   dx.doi.org/10.1021/ic202373a | *Inorg. Chem.* 2012, 51, 4116−4122

Contrarily, when they are on the opposite side, the conformation is defined as anti (Scheme 1). Conformational change is a common, but significant, phenomenon in biological systems.[7] Moreover, conformational change is also an important phenomenon in coordination polymers and organic catalytic systems.[8] Therefore, it is an important topic that is worth paying attention to. In this work, we report an interesting conformational change in discrete coordination cages as well as their characteristics in the solid state and/or solution.

Scheme 1. Two Conformations of the Ligand TPPA Observed in the Cages: (I) Syn and (II) Anti

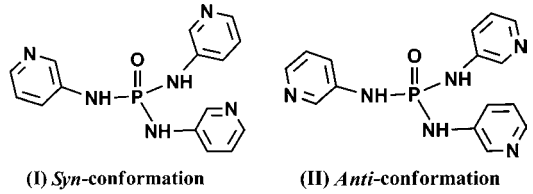

EXPERIMENTAL SECTION

General Details. TPPA was prepared according to the procedures outlined in the literature.[9] All other reagents were obtained from commercial vendors and, unless otherwise noted, were used without further purification. ***Caution!*** *Perchlorate salts of metal complexes with organic ligands are potentially explosive. Only a small amount of material should be prepared, and it should be handled with care.* Emission and excitation spectra were recorded on an Edinburgh Instruments FLS920 spectrofluorimeter equipped with both continuous-wave (450 W) and pulse xenon lamps. IR spectra were recorded with KBr pellets on a Perkin-Elmer Spectrum One FT-IR spectrometer in the range 400−4000 cm^{-1}. Single-crystal X-ray diffractions were carried out by the 4W2 High Pressure Station of Beijing Synchrotron Radiation Facility (BSRF) and a Saturn 70 charge-coupled-device diffractometer. Elemental analyses for C, H, and N were carried out on a Vario EL III elemental analyzer. The powder X-ray diffraction (PXRD) patterns were collected using a diffractometer (Rigaku DMAX2500) with Cu Kα radiation (λ = 1.5406 Å).

Synthesis of $[Ni_6(TPPA)_8(H_2O)_{12}](ClO_4)_{12}\cdot 57H_2O$ (1). $Ni(ClO_4)_2\cdot 6H_2O$ (0.022 g, 0.06 mmol) and TPPA (0.026 g, 0.08 mmol) were added to a mixed solvent of tetrahydrofuran (THF), ethanol (EtOH), and water (H_2O; 9 mL; 1:1:1, v/v/v), and this mixture was sealed in a 30-mL Teflon-lined autoclave. The autoclave was heated to 120 °C, held for 72 h, and cooled to room temperature at a rate of 0.1 °C/min. Slightly blue cubic single crystals of **1** were collected and washed with 5 mL of *n*-hexane. Yield: 68%. Elem anal. Calcd for $C_{120}H_{258}N_{48}O_{125}Cl_{12}P_8Ni_6$: C, 26.69; H, 4.82; N, 12.45. Found: C, 26.75; H, 4.72; N, 12.42. IR data (KBr, cm^{-1}): 3506(w), 3263(s), 1586(m), 1501(s), 1393(s), 1335(w), 1271(s), 1103(s), 962(s), 809(m), 704(m), 625(s), 498(w).

Synthesis of $[Co_6(TPPA)_8(H_2O)_{12}](ClO_4)_{12}\cdot 57H_2O$ (2). Compound **2** was prepared by a procedure similar to that used for the preparation of compound **1** except that $Co(ClO_4)_2\cdot 6H_2O$ (0.022 g, 0.06 mmol) was used instead of $Ni(ClO_4)_2\cdot 6H_2O$. Yield: 64%. Eleme anal. Calcd for $C_{120}H_{258}N_{48}O_{125}Cl_{12}P_8Co_6$: C, 26.70; H, 4.78; N, 12.45. Found: C, 27.04; H, 4.68; N, 12.58. IR data (KBr, cm^{-1}): 3512(w), 3294(s), 1575(s), 1468(s), 1396(s), 1329(w), 1269(s), 1185(m), 1106(s), 951(s), 816(m), 635(m), 495(w).

Synthesis of $[Zn_6(TPPA)_8(H_2O)_{12}](ClO_4)_{12}\cdot 57H_2O$ (3). Compound **3** was prepared by a procedure similar to that used for the preparation of compound **1** except that $Zn(ClO_4)_2\cdot 6H_2O$ (0.022 g, 0.06 mmol) was used instead of $Ni(ClO_4)_2\cdot 6H_2O$. Yield: 56%. Elem anal. Calcd for $C_{120}H_{258}N_{48}O_{125}Cl_{12}P_8Zn_6$: C, 26.50; H, 4.78; N, 12.36. Found: C, 26.74; H, 4.58; N, 12.42. IR data (KBr, cm^{-1}): 3516(w), 3270(s), 1588(s), 1392(s), 1336(m), 1272(s), 1194(w), 1090(s), 966(s), 810(m), 622(m), 492(w). ^1H NMR (400 MHz, DMSO-d_6, TMS): δ 8.43 (s, 3H, d), 8.08 (d, 3H, c), 7.57 (d, 3H, a), 7.23 (q, 3H, b) (Figure S5 in the Supporting Information). ^{31}P NMR (161.9 MHz, DMSO-d_6): δ −4.29 (Figure S6 in the Supporting Information).

Synthesis of $[Cd_6(TPPA)_8(H_2O)_{12}](ClO_4)_{12}\cdot 57H_2O$ (4). Compound **4** was prepared by a procedure similar to that used for the preparation of compound **1** except that $Cd(ClO_4)_2\cdot 6H_2O$ (0.025 g, 0.06 mmol) was used instead of $Ni(ClO_4)_2\cdot 6H_2O$. Yield: 63%. Elem anal. Calcd for $C_{120}H_{258}N_{48}O_{125}Cl_{12}P_8Cd_6$: C, 25.19; H, 4.55; N,

Table 1. Crystallographic Data and Details of Refinements for Compounds 1−5

	1	2	3	4	5
formula	$C_{120}H_{258}N_{48}O_{125}Cl_{12}P_8Ni_6$	$C_{120}H_{120}N_{48}O_{68}Cl_{12}P_8Co_6$	$C_{120}H_{120}N_{48}O_{20}P_8Zn_6$	$C_{120}H_{120}N_{48}O_{20}P_8Cd_6$	$C_{120}H_{48}N_{48}O_{28}Cl_{12}P_8Pd_6$
fw	5398.99	4349.38	3194.62	3476.8	3921.62
temp (K)	173(2)	173(2)	298(2)	298(2)	293(2)
wavelength (Å)	0.70000	0.71073	0.71073	0.71073	0.71073
cryst syst	cubic	cubic	cubic	cubic	tetragonal
space group	$I\bar{4}3d$	$I\bar{4}3d$	$I\bar{4}3d$	$I\bar{4}3d$	$I4/mmm$
a (Å)	45.214(5)	45.317(5)	45.239(2)	45.702(6)	20.9346(2)
b (Å)	45.214(5)	45.317(5)	45.239(2)	45.702(6)	20.9346(2)
c (Å)	45.214(5)	45.317(5)	45.239(2)	45.702(6)	28.252(4)
α (deg)	90	90	90	90	90
β (deg)	90	90	90	90	90
γ (deg)	90	90	90	90	90
volume (Å^3)	92431(3)	93064(3)	92585(7)	95457(2)	12382(2)
Z	16	16	16	16	2
D_c (Mg/m^3)	1.552	1.242	0.917	0.968	1.052
μ (mm^{-1})	0.787	0.662	0.717	0.630	0.660
data collected	39903	74872	314617	357796	43138
unique data (R_{int})	13517	19238	17634	18248	3376
parameters	1007	790	607	602	170
GOF on F^2	1.028	1.013	1.070	1.009	1.039
R1[a] [$I > 2\sigma(I)$]	0.0856	0.0955	0.0930	0.0734	0.0803
wR2[b]	0.2498	0.3061	0.2756	0.2258	0.2764

[a] $R1 = \sum||F_o| - |F_c||/\sum|F_o|$. [b] $wR2 = \{\sum[w(F_o^2 - F_c^2)^2]/\sum[w(F_o^2)^2]\}^{1/2}$.

dx.doi.org/10.1021/ic202373a | Inorg. Chem. 2012, 51, 4116−4122

11.75. Found: C, 25.53; H, 4.34; N, 11.95. IR data (KBr, cm^{-1}): 3504(w), 3287(s), 1588(s), 1470(s), 1390(s), 1334(w), 1270(s), 1194(m), 1108(s), 954(s), 804(m), 626(m), 492(w). ^{1}H NMR (400 MHz, DMSO-d_6, TMS): δ 8.45 (s, 3H, d), 8.08 (d, 3H, c), 7.56 (d, 3H, a), 7.24 (q, 3H, b) (Figure S5 in the Supporting Information). ^{31}P NMR (161.9 MHz, DMSO-d_6): δ −4.29 (Figure S6 in the Supporting Information).

Synthesis of $[Pd_6(TPPA)_8]Cl_{12}\cdot 22H_2O$ (5). Compound **5** was prepared by layering a solution of TPPA (0.026 g, 0.08 mmol) in 5 mL of methanol onto a solution of K_2PdCl_4 (0.020 g, 0.06 mmol) in 10 mL of *N*,*N*-dimethylformamide (DMF). After 4 weeks, pure colorless crystals suitable for X-ray crystallographic analysis were harvested. Yield: 43%. Elem anal. Calcd for $C_{120}H_{164}N_{48}O_{30}Cl_{12}P_8Pd_6$: C, 35.41; H, 4.06; N, 16.52. Found: C 35.57, H 4.12; N, 16.76. IR data (KBr, cm^{-1}): 3431(m), 3046(m), 2955(w), 2862(w), 1666(w), 1582(m), 1479(s), 1252(s), 963(s), 829(w), 695(m), 505(w). ^{1}H NMR (400 MHz, DMSO-d_6, TMS): δ 8.52 (s, 24H, d′), 8.17 (d, 24H, c′), 7.69 (d, 24H, a′), 7.38 (q, 24H, b′). ^{31}P NMR (161.9 MHz, DMSO-d_6): δ −4.20. ESI-MS: m/z 269.7 ($[M - 12Cl^-]^{12+}$), 331.0 ($[M - 10Cl^-]^{10+}$), 488.9 ($[M - 7Cl^-]^{7+}$), 576.3 ($[M - 6Cl^-]^{6+}$), 710.4 ($[M - 5Cl^-]^{5+}$).

Single-Crystal Structure Determination. Data for compound **1** was collected by using the 4W2 High Pressure Station of BSRF. Monochromatic radiation at a wavelength of 0.70 Å was adopted for pattern collection. Data for compounds **2**−**5** were collected on a Saturn 70 charge-coupled-device diffractometer equipped with confocal-monochromatized Mo Kα radiation (λ = 0.71073 Å) from a rotating-anode generator. The structures were solved by direct methods and refined on F^2 by full-matrix least-squares methods by using the *SHELXL-97* program package.[10] As usual for cage compounds, crystals in this paper scattered weakly because of the extensive disorder of anions and lots of solvent molecules.[11] The weakness of the data required using a number of restraints and/or constraints to keep the geometries of the anions, aromatic rings, or solvent molecules reasonable. Therefore, no attempt was made to locate the H atoms of the guest molecules. In structures of compounds **2**−**4**, there were extensive areas of residual electron density that could not sensibly be modeled as solvents or anions. Therefore, they were removed via application of the *SQUEEZE* function in *PLATON*. The final formulas of these compounds were determined by combining with elemental analysis. Details of the structure solution and final refinements for the compounds are given in Table 1. CCDC 833817−833821 contain the supplementary crystallographic data (**1**−**5**, respectively) for this paper. These data can be obtained free of charge from The Cambridge Crystallographic Data Centre via www.ccdc.cam.ac.uk/-data_request/cif.

RESULTS AND DISCUSSION

Discrete Octahedral Coordination Cages $[M_6(TPPA)_8(H_2O)_{12}]$ $(ClO_4)_{12}\cdot 57H_2O$ [M = Ni (1), Co (2), Zn (3), Cd (4)]. Single-crystal X-ray diffraction analyses reveal that compounds **1**−**4** are isostructural, and the crystal structure of compound **1** is discussed in detail. The reaction of TPPA and $Ni(ClO_4)_2\cdot 6H_2O$ in a ratio of 4:3 under solvothermal conditions produced high-yield slightly blue cubic single crystals suitable for X-ray crystallographic analysis (Figure 1a). The obtained crystals were soluble in common polar solvents such as methanol, acetonitrile, dimethyl sulfoxide (DMSO), and DMF but insoluble in nonpolar solvents, such as *n*-hexane, cyclohexane, benzene, and trichloromethane. It is worth noting that the crystals of **1**−**4** can also be prepared by reaction of the ligand TPPA and corresponding perchlorate salts in a THF/EtOH/H_2O mixed solvent at room temperature.

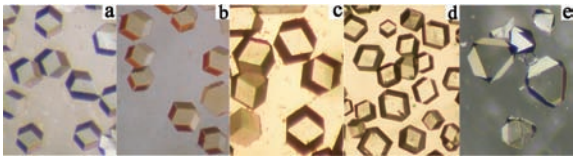

Figure 1. Photographic images of crystals for compounds **1**−**5** (a−e).

The crystals of **1** were weakly diffracted, and X-ray synchrotron radiation was used to collect high-quality data. Compound **1** crystallizes in the high-symmetry cubic space group $I\bar{4}3d$. X-ray crystal structure analysis unambiguously demonstrates that **1** is a discrete Ni_6L_8 cage in octahedral geometry (Figure 2). Eight equivalent TPPA ligands act as three-connected linkers to bridge six Ni^{II} ions at the apexes to form the M_6L_8-type coordination cage. It is interesting that three pyridyl rings on the same TPPA ligand rotate by about 40° with respect to the central P═O groups, which gives the curvature needed for the cage structure. Each Ni^{II} node lies in a distorted octahedral coordination sphere, where the basal plane is defined by four pyridyl N atoms from different TPPA ligands, while the axial positions are occupied by two H_2O molecules. The Ni−N distances range from 2.099(5) to 2.151(4) Å, and the Ni−O distances range from 2.075(4) to 2.126(4) Å. The six Ni^{II} ions in the cage structure occupy the apexes of an imaginary octahedron. The average distance between axially located Ni centers is 13.18 Å, and that between equatorial Ni centers is 9.15 Å. The average distance between the opposite P═O groups situated at the terminus of the 3-fold axis is 12.37 Å. There are three crystallographically imposed 4-fold axes passing through two opposite Ni^{II} centers and four 3-fold axes through P═O groups of the TPPA ligands, which endows the cage with O_h symmetry. It is worth noting that all of the TPPA ligands in compound **1** adopt the syn conformation. The P═O groups of the eight ligands point inward to the center of the cage, which provides a hydrophilic environment inside the cavity. The volume of the internal cavity is estimated to be ca. 900 Å^3.[12] The spherical shape of the cage is important because the cavity volume is maximized. The large internal cavity of the cage offers the possibility of developing a suitable nanosized host system that can accommodate suitable small molecular guests. The other interesting feature of this nanocage is its flexible windows. There are 12 windows on the surface of the cage in each 2-fold axis direction. Each window consists of a 20-membered ring and displays an approximate rectangular shape with the size of 4.3 Å × 7.9 Å (Figure S3 in the Supporting Information). The pyridyl rings can be rotated through a certain angle because of the flexibility of the TPPA ligands, which adjusts the size of the windows to allow anions or suitable molecular guests to enter and leave the cage. Crystallographic analysis demonstrates that the inner cavity of the cage is occupied by free H_2O molecules, while the ClO_4^- anions are located between the cages. In compound **1**, each octahedral cage has 12 nearest neighbors, and they stack themselves in the fashion of the cubic close packing (Figure 2d).

Truncated Octahedral Coordination Cage 5. Compound **5** was prepared with a synthetic procedure different from that of compounds **1**−**4**. Layering a methanol solution of TPPA (0.8 mmol) onto a DMF solution of K_2PdCl_4 (0.6 mmol) yielded colorless block single crystals suitable for X-ray crystallographic analysis (Figure 1e). Compound **5** crystallizes in tetragonal space group $I4/mmm$. Crystal structural analysis demonstrates that **5** is a discrete Pd_6L_8 cage in truncated octahedral geometry (Figure 3). Similar to cage **1**, eight tripodal TPPA ligands are connected at six Pd^{II} ions. Each Pd^{II} ion

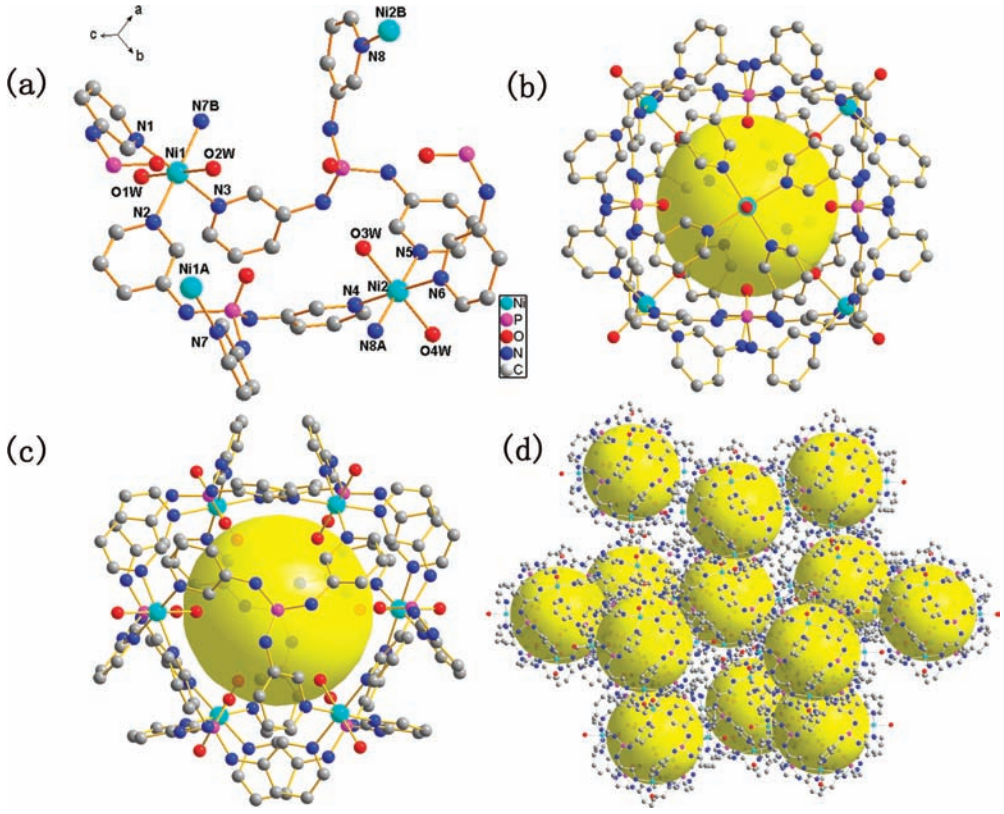

Figure 2. (a) Coordination environment of the Ni^{II} ions and linkage mode of the ligands in **1**. Symmetry codes: A, $1 - z$, $0.5 + x$, $1.5 - y$; B, $-0.5 + y$, $1.5 - z$, $1 - x$. (b) Crystal structure of cage **1** viewed along the 4-fold axis. (c) Crystal structure of cage **1** viewed along the 3-fold axis. (d) Packing diagram of **1** shown as a ball-and-stick model.

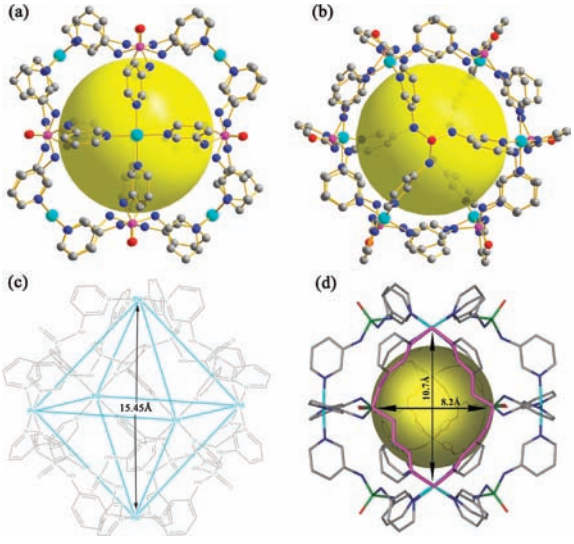

Figure 3. Crystal structure of cage **5**: viewed along the 4-fold axis (a) and along the 3-fold axis (b). (c) Octahedral internal cavity. (d) Rhomboidal windows on the surface of the cage.

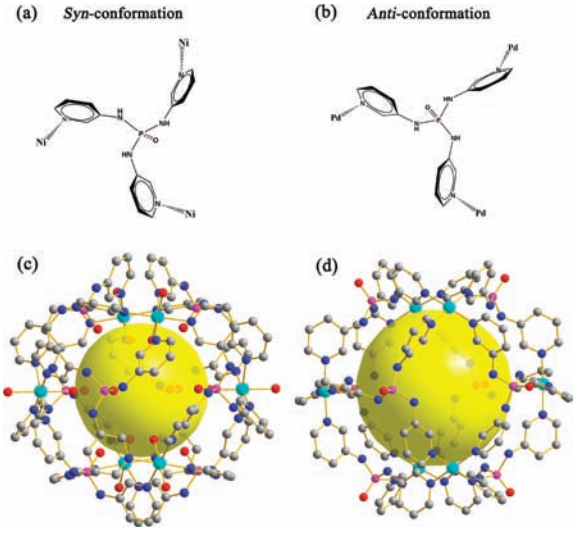

Figure 4. Two conformations of TPPA observed in cages **1** and **5**: (a) syn and (b) anti. The cage structures of **1** (c) and **5** (d) constructed with syn and anti forms of ligands, respectively.

adopts a C_4-symmetric square-planar coordination geometry, which is defined by four pyridyl donors. The Pd−N distances range from 2.012(4) to 2.021(6) Å. The coordination environment of the TPPA ligand is very similar to that in cage **1**. However, the orientation of the central P═O group is different from that in cage **1**. In compound **5**, all TPPA ligands adopt an anti conformation, with all P═O groups pointing outward from the inner cavity of the cage (Figure 4). It is notable that when the pyridyl rings rotate by about 180°, the TPPA ligand can transform from syn to anti conformation. As in cage **1**, cage **5** has 12 rhomboidal windows on the surface of the cage structure. It is interesting that the window size is remarkably increased to 10.7 Å × 8.2 Å because of conformational change (Figure 5). Furthermore, the distance of the axial metal centers is 15.45 Å, which is 2.27 Å longer than that in cage **1**. Therefore, cage **5** with anti-conformational

dx.doi.org/10.1021/ic202373a | *Inorg. Chem.* 2012, 51, 4116−4122

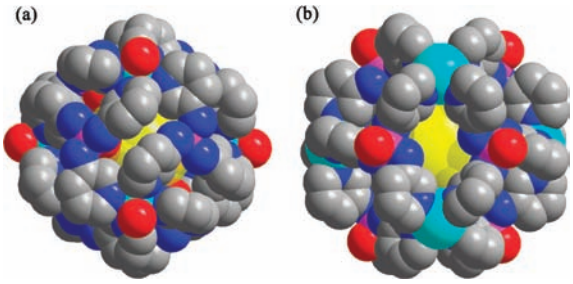

Figure 5. Space-filling models of cage **1** (a) and cage **5** (b) showing a remarkable enhancement of the window size via conformational change. Color code: cyan, nickel/palladium; red, oxygen; blue, nitrogen; gray, carbon; magenta, phosphorus; yellow, dummy atom.

ligands has a slightly increased cavity volume (~1300 Å^3). Interestingly, the Cl ions act as counteranions and are positioned in the cavity of the cage molecules. The increase in both the windows and the internal cavity will allow larger guest molecules or anions to enter and leave the cage. To our knowledge, there are several factors that would lead to conformational change of the flexible ligands, including reaction conditions, steric hindrances, hydrogen-bonding interactions, and solvent effect.[13] As described previously, crystals of **1**–**4** with syn-conformational ligands can be obtained at different temperatures, suggesting that the temperature is not a factor in determining the conformations. On the basis of our previous studies, we know that a kind of counteranion does not affect the resultant supramolecular structure basically.[9] Therefore, we believe that the solvent effect may be the most probable factor in determining the conformation of the ligand in the molecular cages. ^{31}P NMR spectroscopy may be helpful for understanding conformational change. Thus, we performed ^{31}P NMR spectroscopy of compound **4** dissolved in different solvents including DMSO-d_6, DMF, D_2O, and MeOH (Figure S7 in the Supporting Information). A single peak with different chemical shifts was observed in each spectrum. On the basis of the number of signals and different chemical shifts in the ^{31}P NMR spectra, it is known that the solvents can influence the resultant structure and the solvent effect may be the most probable factor for conformational change.

Solution NMR and Mass Spectrometry Studies. Both NMR spectroscopy and electrospray ionization mass spectrometry (ESI-MS) are very helpful for providing information on the structural integrity of the complexes in solution and especially helpful for confirming structures that cannot be directly determined by single-crystal X-ray diffraction.[14] All of the synthesized compounds were characterized by NMR spectroscopy and ESI-MS. The results reveal that only compound **5** maintains its structural integrity in solution (Figures 6, 7, and S5 and S6 in the Supporting Information).

First, 0.04 mmol of the TPPA ligand was dissolved in 2 mL of DMSO-*d*6 at room temperature, and the solution was monitored by NMR spectroscopy (Figure 6b). Four singlet signals corresponding to the four kinds of H atoms in the pyridyl rings of the free ligand were observed. Second, 0.03 mmol of K_2PdCl_4 was added to the solution with vigorously stirring, and the solution was directly monitored by NMR spectroscopy after 1 h. Four new signals appeared with a downfield shift in an integral ratio of 1:1:1:1 (Figure 6c). The new signals corresponded to the H atoms of those ligands combined with the Pd^{II} ions, and the downfield of the signals was ascribed to the metal–ligand complexation.[15] In the following 9 h, signals observed for the combined ligands became stronger, implying that more ligands were assembled into the assumed structure (Figure 6d). However, after 10 h, the spectrum did not change significantly with time. Because there is only one set of four new signals corresponding to the pyridyl groups observed in the spectrum, all eight TPPA ligands are equivalent to each other. Therefore, the molecule has 4-fold symmetry in solution. Furthermore, the result also reveals that all eight TPPA ligands have internal symmetry with three equivalent arms. Thus, the molecule has 3-fold axes through the central P═O groups of the opposite TPPA ligands. Deduced from the above result, the cage has O_h symmetry in solution. NMR spectroscopy unambiguously confirmed the integrity of the cage structure of compound **5**. In addition, the ^{1}H NMR spectrum of crystalline **5** in DMSO-d_6 was also studied (Figure

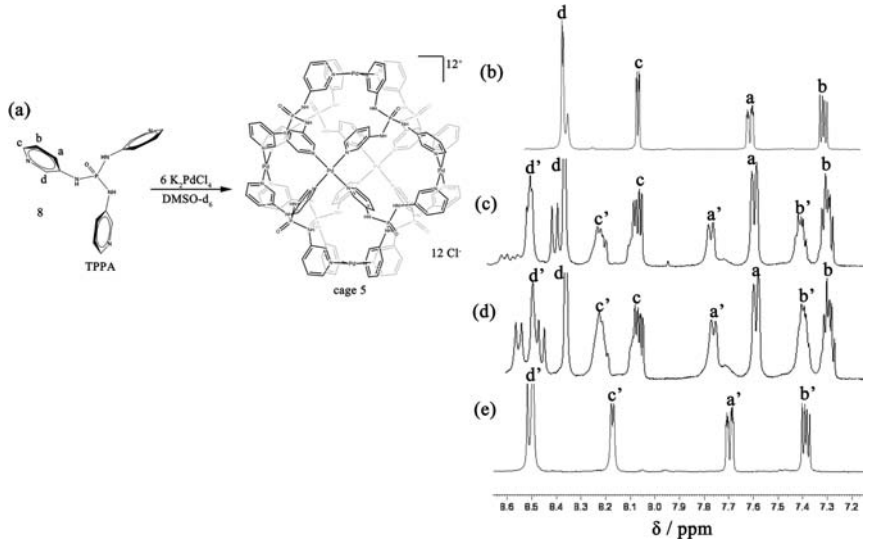

Figure 6. (a) Schematic representation of the preparation of cage **5** via the self-assembly of the anti-form ligand TPPA and K_2PdCl_4. (b) Partial ^{1}H NMR spectrum (400 MHz, rt) of free ligand TPPA in DMSO-d_6. (c) Partial ^{1}H NMR spectrum of the reaction product in 1 h. (d) Partial ^{1}H NMR spectrum of the reaction product in 10 h. (e) Partial ^{1}H NMR spectrum of crystalline **5** dissolved in DMSO-d_6.

dx.doi.org/10.1021/ic202373a | *Inorg. Chem.* 2012, 51, 4116–4122

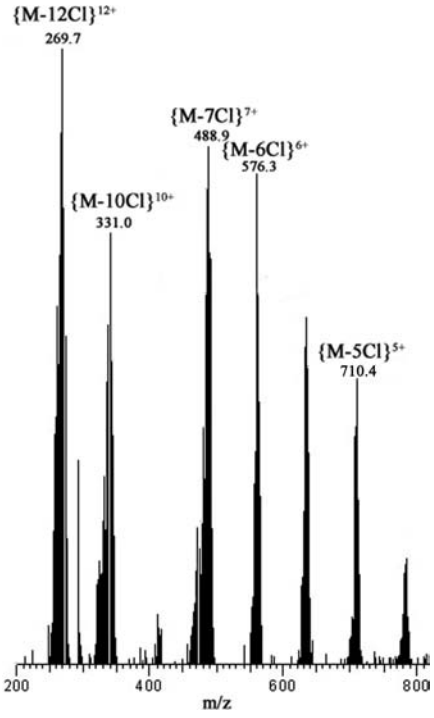

Figure 7. ESI-MS spectrum of compound **5** showing a sequence of peaks corresponding to the species $\{[Pd_6(TPPA)_8]Cl_{12-n}\}^{n+}$ (n = 12, 10, 7, 6, 5).

6e). Four signals corresponding to the protons of the pyridyl ring were observed with a downfield shift compared to the free ligand, which is consistent with the result of the in situ ^{1}H NMR spectrum of **5**.

ESI-MS study on the Pd^{II} cage provided complete confirmation of the structural integrity of compound **5** in solution (Figure 7). For $[Pd_6(TPPA)_8]Cl_{12}$, we observed a clear sequence of peaks at m/z 269.7, 331.0, 488.9, 576.3, and 710.4, which corresponds to the species $\{[Pd_6(TPPA)_8]Cl_{12-n}\}^{n+}$ (n = 12, 10, 7, 6, 5). There are also several unassigned peaks in the MS spectrum, which may correspond to the fragments of the cage structure.

Photoluminescent Properties. Crystal photographs of compound **3** show that it exhibits strong blue emission under UV irradiation (Figure S8 in the Supporting Information). The result can be further confirmed by the luminescent spectra. The solid-state luminescent spectra of the free TPPA ligand and compounds **3** and **4** were investigated at room temperature. The free TPPA exhibits a broad fluorescent emission band at 457 nm under excitation at 365 nm. Compounds **3** and **4** exhibit strong blue emission bands at 398 nm (λ_{ex} = 344 nm) and 407 nm (λ_{ex} = 342 nm), respectively, which are slightly blue-shifted compared with the free ligand (Figure 8). Because the Zn^{II} and Cd^{II} ions are difficult to oxidize or reduce, the emission of these compounds is neither metal-to-ligand charge transfer nor ligand-to-metal charge transfer.[16] The emission of **3** and **4** can probably be attributed to the intraligand or ligand-to-ligand charge transition. It is worth noting that the emission intensity of compounds **3** and **4** increases remarkably and is approximately 1 order of magnitude higher than that of the free ligand. Generally, the enhanced fluorescence efficiency is attributed to coordination of the TPPA ligands to Zn^{II} or Cd^{II} centers, which effectively increases the conformational rigidity of the ligand and reduces thermal vibrations, thereby

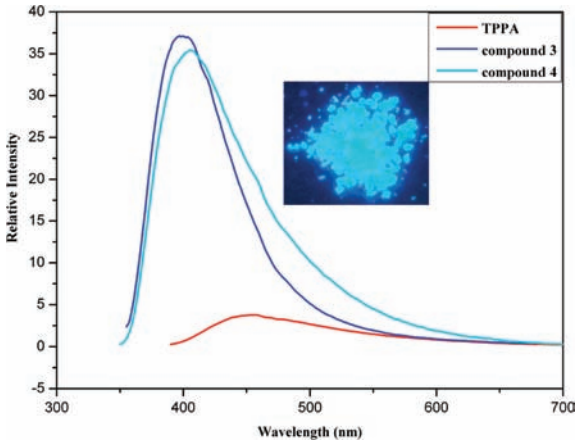

Figure 8. Solid-state emission spectra of the free TPPA ligand and compounds **3** and **4** at room temperature. Inset: Crystal photograph of **3** under UV irradiation.

reducing the nonradiative decay of the intraligand ($\pi-\pi^*$) excited state.[17] To the best of our knowledge, such a remarkable enhancement was rarely reported for the ligand-based luminescent molecular cages or metal−organic frameworks.[18] These photoluminescent properties suggest that compounds **3** and **4** might be good candidates as photoactive materials.

CONCLUSION

In conclusion, we have successfully synthesized five discrete nanosized M_6L_8 coordination cages from a conformationally flexible ligand and transition-metal ions. The nanocages have an octahedral structure with a large internal cavity and 12 flexible windows. The flexible ligand TPPA transforms its conformation from the syn form in cages **1**−**4** to the anti form in cage **5**. Because of the conformational transformation, the sizes of the windows and the volume of the internal cavity of cage **5** are increased. ^{1}H NMR and ESI-MS studies reveal that cage **5** maintains its structural integrity in solution. Compared with the free ligand, strong blue emissions with an unexpected great enhancement are observed for compounds **3** and **4**. This research may provide a promising approach to obtain new high-symmetry coordination cages. Further studies will focus on exploring guest encapsulation and the catalytic properties of the synthesized cage compounds.

ASSOCIATED CONTENT

Supporting Information

Crystallographic data (CIFs; CCDC 833817−833821 for **1**−**5**), IR and NMR spectra, PXRD patterns, additional structural figures, and selected bond lengths (Å) and bond angles (deg) for **1** and **5**. This material is available free of charge via the Internet at http://pubs.acs.org.

AUTHOR INFORMATION

Corresponding Author

*E-mail: hmc@fjirsm.ac.cn. Tel.: +86 591 83792460. Fax: +86 591 83714946.

Notes

The authors declare no competing financial interest.

■ ACKNOWLEDGMENTS

We gratefully acknowledge financial support by the 973 Program (Grants 2011CB932504 and 2011CBA00507), National Science Foundation of China (Grant 21131006), and National Science Foundation Fujian Province. We are also grateful to Prof. Xiao-Ying Huang for the crystal data refinement.

■ REFERENCES

(1) (a) Cram, D. J. *Nature* **1992**, *356*, 29−36. (b) Liu, X.; Chu, G.; Moss, R. A.; Sauers, R. R.; Warmuth, R. *Angew. Chem., Int. Ed.* **2005**, *117*, 2030−2033. (c) Sawada, T.; Yoshizawa, M.; Sato, S.; Fujita, M. *Nat. Chem.* **2009**, *1*, 53−56. (d) Ono, K.; Yoshizawa, M.; Akita, M.; Kato, T.; Tsunobuchi, Y.; Ohkoshi, S.; Fujita, M. *J. Am. Chem. Soc.* **2009**, *131*, 2782−2783. (e) Trembleau, L.; Rebek, J. Jr. *Science* **2003**, *301*, 1219−1220. (f) Therrien, B.; Süss-Fink, G.; Govindaswamy, P.; Renfrew, A. k.; Dyson, P. J. *Angew. Chem., Int. Ed.* **2008**, *120*, 3833−3836. (g) Dong, V.-M.; Fiedler, D.; Carl, B.; Bergman, R. G.; Raymond, K. N. *J. Am. Chem. Soc.* **2006**, *128*, 14464−14465. (h) Osuga, T.; Murase, T.; Ono, K.; Yamauchi, Y.; Fujita, M. *J. Am. Chem. Soc.* **2010**, *132*, 15553−15555. (i) Zhang, J.-P.; Chen, X.-M. *J. Am. Chem. Soc.* **2009**, *131*, 5516−5521. (j) Dalgarno, S. J.; Power, N. P.; Atwood, J. L. *Coord. Chem. Rev.* **2008**, *252*, 825−841. (k) Clever, G. H.; Tashiro, S.; Shionoya, M. *Angew. Chem., Int. Ed.* **2009**, *48*, 7010−7012.

(2) (a) Zava, O.; Mattsson, J.; Therrien, B.; Dyson, P. *Chem.—Eur. J.* **2010**, *16*, 1428−1431. (b) Turner, J. L.; Wooley, K. L. *Nano Lett.* **2004**, *4*, 683−688. (c) Pan, D.; Turner, J. L.; Wooley, K. L. *Chem. Commun.* **2003**, 2400−2401. (d) Zhao, D.; Tan, S.-W.; Yuan, D.-Q.; Lu, W.-G.; Rezenom, Y. H.; Jiang, H.-L.; Wang, L.-Q.; Zhou, H.-C. *Adv. Mater.* **2011**, *23*, 90−93.

(3) (a) Murase, T.; Horiuchi, S.; Fujita, M. *J. Am. Chem. Soc.* **2010**, *132*, 2866−2867. (b) Nishioka, Y.; Yamaguchi, T.; Kawano, M.; Fujita, M. *J. Am. Chem. Soc.* **2008**, *130*, 8160−8161. (c) Hastings, C. J.; Pluth, M. D.; Bergman, R. G.; Raymond, K. N. *J. Am. Chem. Soc.* **2010**, *132*, 6938−6940. (d) Pluth, M. D.; Bergman, R. G.; Raymond, K. N. *Acc. Chem. Res.* **2009**, *42*, 1650−1659. (e) Pinacho Crisóstomo, F. R.; Rebek, J. Jr. *J. Am. Chem. Soc.* **2009**, *131*, 7402−7410. (f) Leung, D. H.; Bergman, R. G.; Raymond, K. N. *J. Am. Chem. Soc.* **2006**, *128*, 9781−9797. (g) Noh, T. H.; Heo, E.; Park, K. H.; Jung, O. S. *J. Am. Chem. Soc.* **2011**, *133*, 1236−1239. (h) Koblenz, T. S.; Wassenaar, J.; Reek, J. N. H. *Chem. Soc. Rev.* **2008**, *37*, 247−262.

(4) (a) Zheng, S.-T.; Bu, J.-T.; Li, Y.; Wu, T.; Zuo, F.; Feng, P.; Bu, X. *J. Am. Chem. Soc.* **2010**, *132*, 17062−17064. (b) Ajami, D.; Rebek, J. Jr. *Angew. Chem., Int. Ed.* **2008**, *47*, 6059−6061. (c) Sava, D. F.; Kravtsov, V. C.; Eckert, J.; Eubank, J. F.; Nouar, F.; Eddaoudi, M. *J. Am. Chem. Soc.* **2009**, *131*, 10394−10396. (d) Li, J.-R.; Zhou, H.-C. *Nat. Chem.* **2010**, *2*, 893−898. (e) Prakash, M. J.; Oh, M.; Liu, X.-F.; Han, K. N.; Seong, G. H.; Lah, M. S. *Chem. Commun.* **2010**, *46*, 2049−2051.

(5) (a) Sun, Q.-F.; Iwasa, J.; Ogawa, D.; Ishido, Y.; Sato, S.; Ozeki, T.; Sei, Y.; Yamaguchi, K.; Fujita, M. *Science* **2010**, *328*, 1144−1147. (b) Stephenson, A.; Argent, S. P.; Johannessen, T. R.; Tidmarsh, I. S.; Ward, M. D. *J. Am. Chem. Soc.* **2011**, *133*, 858−870. (c) Meng, W.-J.; Breiner, B.; Rissanen, K.; Thoburn, J. D.; Clegg, J. K.; Nitschke, J. R. *Angew. Chem., Int. Ed.* **2011**, *50*, 3479−3483. (d) Kishi, N.; Li, Z.; Yoza, K.; Akita, M.; Yoshizawa, M. *J. Am. Chem. Soc.* **2011**, *133*, 11438−11441. (e) Dong, Y.-B.; Wang, P.; Ma, J.-P.; Zhao, X.-X.; Wang, H.-Y.; Tang, B.; Huang, R.-Q. *J. Am. Chem. Soc.* **2007**, *129*, 4872−4873. (f) Serra, S. C.; Coronado, E.; Gaviña, P.; Ponce, J.; Tatay, S. *Chem. Commun.* **2011**, *47*, 8235−8237.

(6) (a) Chand, D. K.; Biradha, K.; Fujita, M.; Sakamoto, S.; Yamaguchi, K. *Chem. Commun.* **2002**, 2486−2487. (b) Moon, D.; Kang, S.; Park, J.; Lee, K.; John, R. P.; Won, H.; Seong, G. H.; Kim, Y. S.; Kim, G. H.; Rhee, H.; Lah, M. S. *J. Am. Chem. Soc.* **2006**, *128*, 3530−3531. (c) Hong, M.-C.; Zhao, Y.-J.; Su, W.-P.; Cao, R.; Fujita, M.; Zhou, Z.-Y.; Chan, A. S. C. *J. Am. Chem. Soc.* **2000**, *122*, 4819−4820. (d) Hiraoka, S.; Harano, K.; Shiro, M.; Ozawa, Y.; Yasuda, N.; Toriumi, K.; Shionoya, M. *Angew. Chem., Int. Ed.* **2006**, *45*, 6488−6491. (e) Liu, H.-K.; Tong, X.-J. *Chem. Commun.* **2002**, *12*, 1316−1317. (f) Wang, Y.; Okamura, T.-A.; Sun, W.-Y.; Ueyama, N. *Cryst. Growth Des.* **2008**, *8*, 802−804.

(7) Zhang, Q.; Kang, M.; Peterson, R. D.; Feigon, J. *J. Am. Chem. Soc.* **2011**, *133*, 5190−5193.

(8) (a) Wright, P. A. *Science* **2010**, *329*, 1025−1026. (b) Perry, J. J. IV; Kravtsov, V. C.; McManus, G. J.; Zaworotko, M. *J. Am. Chem. Soc.* **2007**, *129*, 10076−10077. (c) Tureček, F.; Panja, S.; Wyer, J. A.; Ehlerding, A.; Zettergren, H.; Nielsen, S. B.; Hvelplund, P.; Bythell, B.; Paizs, B. *J. Am. Chem. Soc.* **2009**, *131*, 16472−16487. (d) Lindsay, V. N. G.; Lin, W.; Charette, A. B. *J. Am. Chem. Soc.* **2009**, *131*, 16383−16385.

(9) Li, N.; Jiang, F.-L.; Chen, L.; Li, X.-J.; Chen, Q.-H.; Hong, M.-C. *Chem. Commun.* **2011**, *47*, 2327−2329.

(10) (a) Sheldrick, G. M. *SHELX-97, Program for the Refinement of Crystal Structures*; University of Göttingen: Göttingen, Germany, 1997. (b) Sheldrick, G. M. *Acta Crystallogr., Sect. A* **2007**, *64*, 112−112.

(11) (a) Tominaga, M.; Suzuki, K.; Kawano, M.; Kusukawa, T.; Ozeki, T.; Sakamoto, S.; Yamaguchi, K.; Fujita, M. *Angew. Chem., Int. Ed.* **2004**, *43*, 5621−5625. (b) Li, J.-R.; Yakovenko, A. A.; Lu, W.-G.; Timmons, D. J.; Zhuang, W.-J.; Yuan, D.-Q.; Zhou, H.-C. *J. Am. Chem. Soc.* **2010**, *132*, 17599−17610.

(12) van der Waals radii were taken into consideration in all cases (Ni, 1.35; C, 1.70; H, 1.20; O, 1.52; N, 1.55; P, 1.80). The yellow dummy ball represents the size of the largest molecule that may occupy the cage without contacting the van der Waals internal surface.

(13) (a) Wang, J.; Zhang, Y.-H.; Tong, M.-L. *Chem. Commun.* **2006**, 3166−3168. (b) Bi, W.-H.; Cao, R.; Sun, D.-F.; Yuan, D.-Q.; Li, X.; Wang, Y.-Q.; Li, X.-J.; Mao, C.-H. *Chem. Commun.* **2004**, 2104−2105. (c) Songkram, C.; Ohta, K.; Yamaguchi, K.; Pichierri, F.; Endo, Y. *Inorg. Chem.* **2010**, *49*, 11174−11183.

(14) (a) Olenyuk, B.; Whiteford, J. A.; Fechtenkötter, A.; Stang, P. J. *Nature* **1999**, *398*, 796−799. (b) Zheng, Y.-R.; Zhao, Z.; Wang, M.; Ghosh, K.; Pollock, J. B.; Cook, T. R.; Stang, P. J. *J. Am. Chem. Soc.* **2010**, *132*, 16873−16882. (c) Al-Rasbi, N. K.; Tidmarsh, I. S.; Argent, S. P.; Adams, H.; Harding, L. P.; Ward, M. D. *J. Am. Chem. Soc.* **2008**, *130*, 11641−11649. (d) Zuccaccia, D.; Pirondini, L.; Pinalli, R.; Dalcanale, E.; Macchioni, A. *J. Am. Chem. Soc.* **2005**, *127*, 7025−7032.

(15) (a) Wang, M.; Zheng, Y.-R.; Ghosh, K.; Stang, P. J. *J. Am. Chem. Soc.* **2010**, *132*, 6282−6283. (b) He, Q.-T.; Li, X.-P.; Yu, Z.-Q.; Wang, W.; Su, C.-Y. *Angew. Chem., Int. Ed.* **2009**, *48*, 6156−6159.

(16) (a) Lin, J.-G.; Zang, S.-Q.; Tian, Z.-F.; Li, Y.-Z.; Xu, Y.-Y.; Zhu, H.-Z.; Meng, Q.-J. *CrystEngComm* **2007**, *9*, 915−921. (b) Wen, L.-L.; Li, Y.-Z.; Lu, Z.-D.; Lin, J.-G.; Duan, C.-Y.; Meng, Q.-J. *Cryst. Growth Des.* **2006**, *6*, 530−537. (c) Wen, L.-L.; Lu, Z.-D.; Lin, J.-G.; Tian, Z.-F.; Zhu, H.-Z.; Meng, Q.-J. *Cryst. Growth Des.* **2007**, *7*, 93−99.

(17) Allendorf, M. D.; Bauer, C. A.; Bhakta, R. K.; Houk, R. J. T. *Chem. Soc. Rev.* **2009**, *38*, 1330−1352.

(18) Zhao, J.; Wang, X.-L.; Shi, X.; Yang, Q.-H.; Li, C. *Inorg. Chem.* **2011**, *50*, 3198−3205.